Carbon−Deuterium Vibrational Probes of the Protonation State of Histidine in the Gas-Phase and in Aqueous Solution

C. S. Miller and S. A. Corcelli*

Department of Chemistry and Biochemistry, University of Notre Dame, Notre Dame, Indiana 46556

Received: March 30, 2010; Revised Manuscript Received: May 14, 2010

The protonation state of ionizable residues is an important contributor to protein stability and function. Histidine is of particular importance because its side chain pK_a is near physiological pH. The sensitivity of carbon deuterium (C−D) vibrational frequencies to the protonation state of histidine dipeptide (Hdp) was investigated in the gas-phase using density functional theory (DFT) calculations, and in aqueous solution using two-layered integrated molecular orbital and molecular mechanics (ONIOM) calculations. All three C−D vibrational probes on the side chain (C_β−D_2, C_δ−D, and C_ε−D) independently exhibited a striking sensitivity to the gas-phase histidine protonation state, with calculated shifts of up to 40 cm^{-1} upon deprotonation of the histidine residue. Simultaneously including all three C−D vibrational probes on the Hdp side chain produced significant shifts of 28 to 43 cm^{-1} between the neutral and charged states. The calculated intensities also dropped precipitously upon deprotonation, which is an important factor for the interpretation of experiments employing C−D vibrational probes to investigate side chain protonation. Solvating the labeled Hdp molecule produces an overall blue-shift in the average C−D vibrational frequencies relative to the gas-phase. The C_β−D_2, C_δ−D, and C_ε−D vibrational probes all showed sensitivity to the histidine protonation state, with shifts of up to 40 cm^{-1} in the mean frequencies after deprotonation, which bodes well for studies employing C−D probes to study histidine protonation state in peptides and proteins.

I. Introduction

Changes in protonation state of titratable residues play a critical role in biological structure and function, including protein stability and enzymatic reactivity. Many proteins have thermodynamic stabilities near neutral pH, and will denature at high and low pH partly due to repulsion between newly formed charged sites.[1−8] For example, the deprotonation of lysine and tyrosine residues causes the protein barstar to unfold at pH > 10,[9] while the protein staphylococcal nuclease unfolds at approximately pH = 4 because of the destabilization of segments containing glutamic acid residues.[10] Near neutral pH, histidine ionization, hydrogen bonding, and hydrophobic interactions contribute to protein stability. Histidine is also vital to the functionality of enzymes. For example, the activity of pyruvate decarboxylase depends on a single histidine opening and closing in the active site through electrostatic interaction with the carboxylic group of the pyruvate substrate.[11] The prominence of histidine in biological processes results from several factors, including structural contributions from the aromatic, planar imidazole ring, the ability of deprotonated imidazole nitrogen atoms to bind to metal ions, and, most importantly, the near neutral pK_a of the imidazole group, which allows histidine to act as a general acid or base in enzymatic reactions.[11−15]

The pK_a of titratable residues depends on their local environment: solvent-exposed residues may have pK_a values similar to the species in solution, while the pK_a of buried residues can vary drastically.[2,16,17] This variation makes *a priori* protonation state assignment ambiguous, and it emphasizes the need for additional computational and experimental techniques for the accurate determination of protonation states of titratable residues. Typically, solution NMR has taken advantage of the correlation between protonation state and chemical shifts to experimentally determine the pK_a of buried residues via titrations,[18−20] but this method is not without limitations. First, because of the dependency of protein stability on the interaction between ionizable residues, NMR can only be used with proteins that are not denatured over the pH range of the titration.[1] Additionally, solution NMR can only be applied to globular proteins, making membrane-bound proteins or protein aggregates nearly inaccessible to these experiments.[21]

Infrared (IR) absorption spectroscopy has several attractive features for determining protonation states of ionizable residues in peptides and proteins. Most importantly, vibrational frequencies are exquisitely sensitive to their local environment. In addition, IR spectroscopy offers the possibility of following the dynamics of (de)protonation events with subpicosecond time resolution, and the technique is applicable both to globular proteins in solution and to membrane-bound proteins. Because the IR absorption spectra of proteins are congested, it is generally necessary to utilize site-specific vibrational probes that are decoupled from the native protein vibrational frequencies. Various strategies for introducing unique IR absorbers into proteins have been explored, including isotopic labels (e.g., carbon−deuterium bonds (C−D)[22−43] and isotopically labeled amide groups[44−80]) and the use of nonnative chemical groups (e.g., azide,[81−85] nitrile,[86−108] and thiocyanate[107−110] groups). Each of these approaches offers relative strengths and weaknesses that have been extensively characterized for investigating peptide and protein structure.

Site-specific C−D bonds are particularly promising as reporters of side chain protonation state.[22,23] C−D stretches absorb at an otherwise transparent region of the IR protein spectrum (2100−2300 cm^{-1}) and are decoupled from the other protein modes, allowing them to report exclusively on their local

* To whom correspondence should be addressed. E-mail: scorcell@nd.edu.

10.1021/jp1028596
Published on Web 06/04/2010

environment and/or local conformation. Also, C−D vibrational probes are exceptionally nonperturbative and thus would not be expected to affect the pK_a of nearby titratable sites. Two recent studies, one experimental[22] and one computational,[23] have specifically investigated the sensitivity of C−D vibrational frequencies to the protonation state of titratable amino acids. Weinkam et al. used deuterated lysine residues (Lys-d_8) to study alkaline-induced denaturation in cytochrome *c*.[22] Their approach was to measure the pH at which three specific lysine residues (Lys72, Lys73, and Lys79) deprotonate by observing a shift in their infrared absorption spectra. The success of this strategy requires that the C−D vibrational frequencies respond to changes in their local electrostatic environment caused by the deprotonation event. By assuming that the lysine residues could only deprotonate once they had become solvent accessible, mechanistic insights into alkaline-induced unfolding of cytochrome *c* were obtained by determining the order in which each specific residue deprotonated.

A recent computational study by Miller and Corcelli investigated with gas-phase density functional theory (DFT) calculations the anharmonic vibrational frequencies of C−D_2 probes in arginine, aspartic acid, glutamic acid, and lysine amino acid side chains.[23] Substantial shifts in the symmetric and asymmetric C−D_2 frequencies upon ionization of the amino acid side chains were observed, particularly when the C−D_2 probe was placed immediately adjacent to the titratable group. For example, upon protonation, the symmetric and asymmetric stretch frequencies of a C−D_2 probe placed next to the NH_2 group of a model lysine dipeptide compound shift by 44.9 cm^{-1} and 69.5 cm^{-1}, respectively. Considerably smaller shifts occur when the probe is further from the site of protonation or deprotonation. Interestingly, the predicted harmonic IR absorption intensities also depend sensitively on the protonation state of the nearby acidic or basic group. In general, C−D_2 side chain vibrational probes are predicted to absorb more efficiently in the vicinity of a more negatively charged site. Therefore, C−D_2 vibrations are more intense in the vicinity of deprotonated acidic groups (compared to neutral acidic groups) and neutral basic groups (compared to protonated basic groups). As an example, the predicted intensity of the asymmetric C−D_2 stretch when the probe is placed next to the carboxylic acid group of glutamic acid dipeptide is 6.8 times greater in the deprotonated compound than in the neutral compound.

The previous study by the authors elucidated several broad design and interpretation principles for future experimental studies employing C−D_2 vibrational probes to study the protonation state of acidic and basic amino acid side chains (i.e., the optimal placement of the probe in the side chain and the sensitivity of the intensity of C−D_2 absorbances to the protonation state of the nearby titratable group). However, the potentially important role of aqueous solvation on the C−D_2 vibrational frequencies was not addressed, nor was the sensitivity of C−D probes to the protonation state of histidine residues. The physiologically relevant protonation states for histidine are somewhat more diverse than for arginine, aspartic acid, glutamic acid, and lysine. This is because the imidazole ring of histidine contains two nitrogen atoms (N_δ and N_ε) that can be protonated or deprotonated. In the neutral form of histidine, one of the two nitrogens is protonated, and in the cationic form, both nitrogens are protonated. Furthermore, histidine offers a variety of possible carbon−deuterium labeling strategies. There are two locations on the imidazole ring for C−D labels (C_δ and C_ε) as well as a C_β−D_2 label off of the ring. The goals of the present study are 2-fold: (1) to characterize fully the sensitivity of the various C−D labeling strategies to the protonation states of histidine first in the gas-phase, and (2) to understand the effects of aqueous solvation on the C−D vibrational frequencies. Both of these goals will advance base of fundamental knowledge necessary for the sound design and interpretation of future experiments.

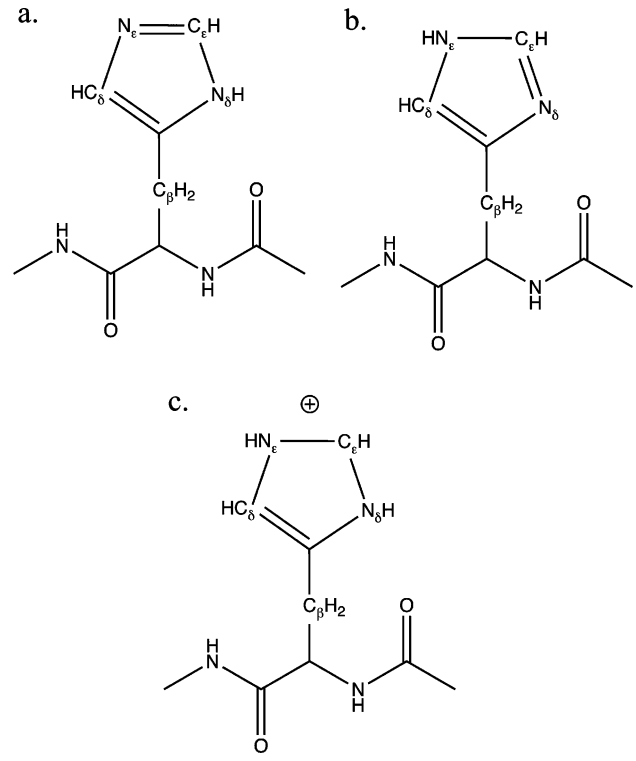

Figure 1. Protonation states of the model histidine dipeptide (Hdp) compound: (a) neutral species protonated at the N_δ site (Hdp N_δ−H), (b) neutral species protonated at the N_ε site (Hdp N_ε−H), and (c) charged species protonated at both the N_δ and N_ε sites (Hdp^+).

In this paper, we present an investigation of the utility of C−D vibrational probes as a reporter of the protonation state of histidine dipeptide (Hdp) in both the gas-phase and in aqueous solution. Details of the Hdp model compound used are provided in Section II-A, while the methodologies used to calculate the anharmonic frequencies of C−D and C−D_2 vibrational probes in the gas- and solution-phases are summarized in Sections II−B and II−C, respectively. In section III-A the sensitivity to histidine protonation state of the gas-phase harmonic and anharmonic vibrational frequencies of three Hdp side chain probes are presented and discussed. Likewise, the results of solution-phase calculations of C−D and C−D_2 labeled Hdp are discussed in Section III−B. Finally, concluding remarks are given in Section IV.

II. Methods

A. Model Histidine Dipeptide (Hdp) Compound. We have investigated the utility of C−D and C−D_2 labels as vibrational probes of the protonation states of the model compound histidine dipeptide (Hdp) using density functional theory (DFT). The two peptide linkages (−CONH-) in Hdp mimic the backbone structure of a larger peptide. As shown in Figure 1, there are three physiologically relevant protonation states of the Hdp side chain. The two neutral species are protonated at either the N_ε or N_δ sites (denoted as Hdp N_ε-H and Hdp N_δ-H, respectively), while the cationic species is protonated at both nitrogen sites. There are three potential locations for a C−D probe on the

TABLE 1: Gas-Phase Vibrational Frequencies of All Three Probes, C_δ−D, C_ε−D, and C_β−D_2, for the Three Protonation States of Hdp: Hdp N_δ-H, Hdp N_ε-H, and Hdp^+, where $\Delta\omega = \omega_{neutral} - \omega_{charged}$[a]

probe	molecule	$\omega_{anharmonic}$ (cm^{-1})		$\Delta\omega_{anharmonic}$ (cm^{-1})		$\omega_{harmonic}$ (cm^{-1})		$\Delta\omega_{harmonic}$ (cm^{-1})		relative intensities	
C_δ−D	Hdp^+	2378.0				2454.2				11.2	
C_δ−D	Hdp N_δ-H	2344.9		−33.1		2411.6		−42.6		6.1	
C_δ−D	Hdp N_ε-H	2357.0		−21.0		2427.7		−26.5		1.0	
C_ε−D	Hdp^+	2373.2				2453.5				26.2	
C_ε−D	Hdp N_δ-H	2348.4		−24.8		2415.4		−38.2		1.0	
C_ε−D	Hdp N_ε-H	2348.8		−24.5		2416.8		−36.8		1.3	
C_β−D_2	Hdp^+	2189.6	2256.8			2221.9	2286.6			1.7	1.0
C_β−D_2	Hdp N_δ-H	2175.4	2235.5	−14.2	−21.3	2209.6	2271.2	−12.3	−15.4	3.9	2.4
C_β−D_2	Hdp N_ε-H	2193.7	2266.4	4.1	9.6	2229.9	2300.3	8.0	13.6	2.6	2.1

[a] For the C_β−D_2 results, the symmetric stretch frequency is on the left and the asymmetric stretch frequency is on the right. All calculations were performed using the B3LYP functional and the aug-cc-pVDZ basis set.

histidine side chain: C_ε−D, C_δ−D, and C_β−D_2. C_δ−D is adjacent to the N_ε protonation site, C_ε−D is between the N_ε and N_δ atoms, and C_β−D_2 is immediately adjacent to the imidazole ring. Previous computational work investigating the properties of carbon−deuterium vibrational probes as reporters of protonation state has focused on C−D_2 probes on the side chains of arginine, aspartic acid, glutamic acid, and lysine model dipeptide compounds in the gas-phase.[23] In the present study, we will explore all three C−D probes of the three Hdp protonation states in both the gas-phase and in aqueous solution. The gas-phase methodology will be described in Section II−B, and the solution-phase methodology in Section II−C.

B. Gas-Phase Methodology. Optimized geometries of the two neutral Hdp compounds, Figure 1a and b, were found in the gas-phase using the B3LYP[111,112] functional and aug-cc-pVDZ[113] basis set, as implemented in Gaussian 03.[114] The B3LYP/aug-cc-pVDZ theory/basis set combination was found to be a reasonable choice for computing C−D_2 vibrational frequencies in our previous study of carbon−deuterium probes of amino acid protonation states.[23]

For our investigation of Hdp in the gas-phase, we have chosen to examine the sensitivity of the C−D and C−D_2 stretch frequencies to the histidine protonation state separately from other effects such as changes in conformation. When the charged species (Hdp^+) was allowed to fully relax, it exhibited a large conformational change at the alpha-carbon in the side chain, breaking an existing hydrogen-bond between the C-terminus carbonyl and the N-terminus amide to form a new hydrogen-bond between the imidazole ring and the N-terminus carbonyl. In addition to unnecessarily complicating the interpretation of the carbon−deuterium frequency calculations, the conformation change that occurs when the gas-phase molecule relaxes is not relevant in aqueous or protein environments. Therefore, a single constraint was utilized to allow the Hdp^+ side chain to relax while preventing the large conformational change. Holding the existing hydrogen-bond within the Hdp backbone fixed at a length of 1.993 Å was the only necessary constraint to eliminate the large conformational change. To ensure the reliability of the harmonic C_ε−D, C_δ−D, and C_β−D_2 frequency calculations on the optimized Hdp^+ molecule, we confirmed that the force on the constrained length was relatively small (0.003 au).

Harmonic normal-mode analyses were performed on all optimized structures, for each of the three deuteration states (C_ε−D, C_δ−D, and C_β−D_2). The harmonic frequencies and relative intensities of the carbon−deuterium stretches are presented in Table 1. Because we are ultimately interested in studying carbon−deuterium vibrational probes of protonation states in aqueous and protein environments, it is necessary to have the ability to calculate the frequency of the C−D stretch when the molecule is not in a local minimum energy structure. To this end, anharmonic C−D, and C−D_2 vibrational frequencies are calculated using previous methodology.[23,26] Briefly, for the one-dimensional C−D probes, the C−D bond is stretched from 0.88 to 1.44 Å in 0.08 Å increments, keeping the rest of the molecule fixed. At each C−D bond length, the energy of the molecule is calculated, thereby generating a Born−Oppenheimer potential energy surface (PES) for the C−D stretch. This potential energy curve is fit to a Morse oscillator:

$$V(r) = D(1 - e^{-\alpha(r-r_0)})^2 + \varepsilon_0 \quad (1)$$

where r_0 is the equilibrium bond length, D is the dissociation energy, α sets the range of the potential, and ε_0 is the zero of energy. The Morse oscillator was chosen because it provides a reasonable description of anharmonic vibrations while having an analytical solution for the energies:

$$E_n = DB(n + {}^1/_2)[2 - B(n + {}^1/_2)] \quad (2)$$

where μ is the reduced mass of the C−D bond, 1.714 amu, and

$$B = \frac{\alpha\hbar}{\sqrt{2\mu D}} \quad (3)$$

The C−D anharmonic frequency is simply $\omega = (E_1 - E_0)/\hbar$.

The two-dimensional C−D_2 probe anharmonic frequency calculation follows a similar protocol. First, both C−D bonds are stretched from 0.88 Å to 1.44 Å in 0.08 Å increments, holding the D-C−D angle fixed, creating a potential energy surface on an 8 × 8 grid. This PES is then fit to a two-dimensional, bilinearly coupled Morse oscillator with the form

$$V(r_1, r_2) = D_1(1 - e^{-\alpha_1(r_1 - r_1^0)})^2 + D_2(1 - e^{-\alpha_2(r_2 - r_2^0)})^2 + c(r_1 - r_1^0)(r_2 - r_2^0) + \varepsilon_0 \quad (4)$$

where r_1 and r_2 are the lengths of the arbitrarily designated C−D bonds. A nonlinear least-squares fitting algorithm is used to determine the following parameters: r_1^0 and r_2^0, the equilibrium bond lengths; D_1 and D_2, the bond dissociation energies; α_1 and α_2, parameters setting the range of the potential; ε_0, the zero of energy; and c, the bilinear coupling constant. The Hamiltonian for bilinearly coupled Morse oscillators is

$$H = \frac{p_1^2}{2\mu} + \frac{p_1^2}{2\mu} + \frac{p_1 p_2 \cos(\theta)}{m_C} + V(r_1, r_2) \quad (5)$$

where p_1 and p_2 are the momenta of the two C−D stretches, μ is the reduced mass of the C−D bond, θ is the D−C−D bond angle, and m_C is the mass of carbon.

In order to calculate the symmetric and asymmetric stretch frequencies, it is necessary to find the three lowest eigenvalues of the Hamiltonian of the vibrational modes. This Hamiltonian is written as a sum of the Hamiltonians for the one-dimensional Morse oscillators and the kinetic and potential coupling between them,

$$H = H(p_1;r_1) + H(p_2;r_2) + \frac{p_1 p_2 \cos\theta}{m_c} + c(r_1 - r_1^0)(r_2 - r_2^0) \quad (6)$$

The Hamiltonian matrix was created within a basis of products of one-dimensional Morse oscillators $|nm\rangle$, where n and m are the respective quantum numbers for the first and second Morse oscillator function. 144 basis functions (with n and m both ranging from 0 to 11) were used; the values of the low energy eigenvalues were invariant to increasing basis size. The Hamiltonian matrix was diagonalized numerically, from which the stretch frequencies are calculated from the lowest three eigenvalues:

$$\omega_{sym} = \frac{\varepsilon_1 - \varepsilon_0}{\hbar}$$
$$\omega_{asym} = \frac{\varepsilon_2 - \varepsilon_0}{\hbar} \quad (7)$$

Both the one-dimensional and two-dimensional frequency calculations assume that the stretching mode(s) of the C−$D_{(2)}$ probe is uncoupled from all other vibrational modes of the molecule, including the D−C−D bend. Previous work has shown that this assumption is reasonable for the C−$D_{(2)}$ probe, and that the one- and two-dimensional Morse oscillators are sensible functions for the PES fit.[23,26]

C. Solution-Phase Methodology. The efficacy of the C−D probe as a detector of protonation state was further investigated for the Hdp molecule in the aqueous solution using an explicit model for the solvent. In solution the molecule is not generally at local energy minimum, therefore it would be incorrect to utilize harmonic normal mode calculations. Instead, anharmonic frequencies of the C−D stretch were calculated for a collection of solute/solvent configurations sampled from a molecular dynamics simulation of Hdp in water. The Amber 9[115] molecular dynamics package was used to collect statistically independent configurations of the solvated Hdp molecule (described by the Amber ff99SB[116] molecular mechanics force field) in its three different protonation states. In the first simulation, the Hdp was protonated at the N_δ site and was solvated with 728 TIP3P water molecules, in a cubic periodic box. The second simulation involved Hdp protonated at the N_ε site and was likewise solvated with 728 water molecules. These simulations were inherently charge neutral. In the third simulation, the Hdp was protonated at both N_δ and N_ε, and was solvated with 816 water molecules. A chlorine ion was included to maintain charge neutrality.

Each of the three systems was equilibrated with the following protocol: first, a minimization using steepest descent and conjugate gradient to remove any steric hindrances caused by solvation, followed by a constant volume defrosting from 0 to 300 K under Langevin temperature control. The system was then run under constant pressure for 200 ps to achieve proper density. The box size was isotropically scaled to match the average volume, taken from the average density from the last 100 ps of the NPT equilibration. Finally, the system was equilibrated under constant volume for 200 ps, and the production run was performed in the NVT ensemble for 25 ns. The C_ε−D, C_δ−D, and C_β−D_2 frequency calculations followed the same protocol as described in the gas-phase, except that the single point energy calculation incorporates solvent effects by using the ONIOM[117] method, as implemented in Gaussian 03. From each of the three simulations, 500 statistically independent snapshots, separated by 50 ps, were sampled for vibrational analysis using ONIOM. In the ONIOM calculations, the Hdp molecule was treated quantum mechanically with density functional theory, B3LYP/6-311++G(d, p), and the aqueous solvent was treated classically with the TIP3P molecular mechanics water model. All of the water molecules in the cubic simulation box were included in the non periodic ONIOM calculations with the center of mass of the Hdp molecule positioned at the middle of the box.

Although we have chosen an explicit, mixed quantum mechanics/molecular mechanics model to describe the effects of aqueous solvation on the carbon−deuterium vibrational frequencies of Hdp, continuum solvation models[118,119] could provide additional physical insight. Continuum solvation models have enjoyed considerable recent success in studying the vibrational properties of peptides.[120−123] In the present context, such models would allow the dielectric constant of the surroundings to be systematically varied over the range that vibrational probes could potentially experience in proteins, from ∼2 in the interior of the protein to ∼80 if the side chain is fully solvent exposed.

III. Results

A. Gas Phase. The C−D vibrational probes are extraordinarily sensitive to the protonation state of the histidine side chain in the gas-phase. The anharmonic stretch frequency of the C_ε−D probe, which is located between the titratable nitrogen sites, responds identically when the charged species is deprotonated to form the N_ε-H and N_δ-H species. Both deprotonations result in a red shift of 25 cm^{-1} (Table 1). This result is unsurprising given the local nature of C−D probes; the N_ε-H and N_δ-H species appear nearly identical to the probe even though the imidazole ring is not strictly symmetric. Additionally, upon deprotonation of the charged species, there is a 25-fold *decrease* in the relative intensities of the charged and neutral species. This result is unexpected because our previous study of C−D_2 probes of the protonation state of basic amino acid side chains (lysine and arginine) predicted an *increase* in the relative absorption intensities upon deprotonation. In contrast, the C_β−D_2 probe, which is adjacent to the histidine ring, does exhibit a small increase in intensity upon deprotonation. Taken together, these results illustrate the profound sensitivity of the absorption intensity of C−D probes to the electronic structure of their environment; the intensities of the C_ε−D and C_δ−D probes on the histidine ring behave qualitatively differently from the C_β−D_2 probe off of the ring. It is important, however, to recognize that our intensity calculations are for Hdp molecules in the gas phase. Solvent effects on the intensities are likely to be important, and are difficult to estimate with currently available theoretical methodologies. Nevertheless, the observed

trends are relevant, assuming the solvent effects on the C−D intensities are of roughly the same magnitude for both the neutral and charges histidine side chains. Therefore, the intrinsic differences in intensities should be taken into account when determining the relative populations of protonated and deprotonated species from an experimental spectrum.

The anharmonic stretch frequency of the C_δ−D probe, located adjacent to the N_ε-H site, responds differently upon deprotonation to the N_ε-H and N_δ-H Hdp molecules. The probe frequency red shifts 33 cm^{-1} upon forming the N_δ-H species, while it only shifts 21 cm^{-1} upon deprotonation to the N_ε-H state. This difference can be attributed to the local nature of the probe. Forming the N_δ-H species from the charged state involves removing the proton on the N_ε site, which is adjacent to the probe, and thus has a greater effect on the C−D frequency. Removing the proton at the more distant site, forming the N_ε-H species, has a smaller effect on the probe's vibrational frequency. The calculated harmonic frequencies show the same trend, and the calculations also provide information on the relative intensity differences between the states. Like the C_ε−D probe, the fully protonated state has the largest intensity. Unlike the C_ε−D probe frequencies, the intensity of the N_δ-H state is significantly larger than its N_ε-H counterpart. This intrinsic difference in intensity, along with the differences in the shifts of the two neutral species, let the C_δ−D probe distinguish the neutral from the charged species, as well as the two neutral species from each other. However, as discussed in more detail in the condensed phase results, the ability of the C_δ−D probe to distinguish the neutral N_δ-H and N_ε-H states is limited to the gas-phase.

In both the harmonic and anharmonic frequency calculations, the C_β−D_2 probe is the least sensitive to the deprotonation of the charged species. This result is unsurprising given the local nature of the carbon−deuterium vibrational probes and the position of the C_β−D_2 probe several atoms away from the protonation site. The most striking response is a blue shift upon deprotonation of the Hdp N_ε-H species, as the other probes respond with a red shift. This blue shift is consistent in both our harmonic and anharmonic calculations, so it is not an artifact of our methodology. In the gas-phase, the red shift upon deprotonation of the Hdp N_δ-H and blue shift upon deprotonation of the Hdp N_ε-H provides a marker to distinguish between the two neutral molecules. Similarly, the splitting between the symmetric and asymmetric stretches decreases upon formation of Hdp N_δ-H and increases when forming Hdp N_ε-H. The change in intensity upon deprotonation, a decrease of approximately 2-fold, is roughly the same for the two neutral species, so while it ought to be taken into account when determining relative populations of the charged and neutral species, it does not aid in the identification of which neutral species is present. Although the C_β−D_2 probe is not as sensitive to the deprotonation of the charged species, the difference in its frequency shifts and the splitting between the symmetric and asymmetric frequencies allows it to differentiate the two neutral species in the gas-phase.

From a synthetic viewpoint, requiring the precise placement of a single deuterium substitution is a nonideal; however, in species like lysine dipeptide, preparing the system with multiple C−D sites drastically reduces the sensitivity of the vibrational probe to different protonation states. Fortuitously, our calculations predict that deuterated histidine does not suffer from this limitation; the sensitivity of multiple probes is not reduced relative to a single probe, as in lysine. Harmonic frequency calculations of the three protonation states in the gas-phase with all three probes (C_ε−D, C_δ−D, and C_β−D_2), forming Hdp-d_4, were performed; the results are presented in Table 2. As expected from the 200 cm^{-1} difference in the chain and the ring vibrational modes, the C_β−D_2 asymmetric and symmetric stretches are effectively completely uncoupled from the ring vibrations. The calculated frequencies of these stretches are identical to the calculation of the Hdp deuterated at only the C_β−D_2 site. In contrast, the two ring vibrations (C_ε−D and C_δ−D) couple to form asymmetric and symmetric stretch modes. These modes are sensitive to the protonation state of the system, showing a large blue shift of 20 cm^{-1} to 40 cm^{-1} upon deprotonation of the charged species. If the only response to the change in protonation state were the change in frequency, it would be sufficient for distinguishing the neutral and charged states; however, other properties also show a response. Unlike the C_β−D_2 probe, which maintains a constant splitting between the asymmetric and symmetric stretch frequencies for all protonation states, the splitting between the stretch frequencies in the coupled C_δ−D and C_ε−D mode increases as the system is deprotonated. The splitting is slightly larger in the Hdp N_ε-H system, although it is a small difference that would likely be averaged out in solution. A more drastic change occurs with the intensity of the harmonic frequencies. The coupled C_δ−D/C_ε−D symmetric mode decreases nearly 14-fold upon deprotonation, while the asymmetric mode decreases an astounding 45-fold. In contrast, the intensities of the C_β−D_2 symmetric and asymmetric modes decrease only 2- and 4-fold. Changes in protonation state represent a significant change in the electronic structure of the ring, so the large change in intensity is consistent with the large change in frequency. While all inherent differences in intensity must be taken into account when determining relative populations of species from experimental data, the large change in intensity for the C_δ−D/C_ε−D mode can also be used to distinguish the protonation states, in addition to the frequency shifts. Thus, in addition to representing a more appealing scenario from a synthetic perspective, having a fully deuterated Hdp side chain provides exquisite sensitivity to the protonation state with regard to the frequency shifts of the C_δ−D/C_ε−D and C_β−D_2 probes, as well as the significant changes in the intensity of the peaks.

TABLE 2: Harmonic Gas-Phase Frequencies of the Coupled C_δD/C_εD Modes in Hdp-d_4, where $\Delta\omega = \omega_{neutral} - \omega_{charged}$[a]

probe	molecule	ω (cm^{-1})		$\Delta\omega$ (cm^{-1})		relative intensities	
C_δD/C_εD	Hdp^+	2450.7	2457.0			83.9	45.8
C_δD/C_εD	Hdp N_δ-H	2408.2	2418.8	−42.5	−38.2	15.7	3.8
C_δD/C_εD	Hdp N_ε-H	2415.6	2428.9	−35.1	−28.1	6.2	1.0

[a] Symmetric stretch frequency is on the left and the asymmetric stretch frequency is on the right. The C_β−D_2 frequencies are omitted from the table because they are nearly identical to the results shown in Table 1.

B. Condensed Phase. The sensitivity of the C_δ−D and C_ε−D probes to the Hdp protonation state is maintained upon solvation in water. The response of both probes' vibrational frequencies to changes in protonation state is qualitatively similar, so for conciseness, only the C_ε−D frequency distributions are shown in Figure 2. The difference between the C_ε−D vibrational frequencies in the neutral and charged Hdp molecules is readily apparent in Figure 2, and the average frequencies and shifts of the C_δ−D and C_ε−D Hdp vibrational probes are summarized in Table 3. The C_δ−D vibrational probe exhibits a slightly larger average frequency red shift upon deprotonation (~40 cm^{-1}) than C_ε−D (~30 cm^{-1}), although the magnitudes of the shifts are similar to those predicted in the gas-phase. This indicates that

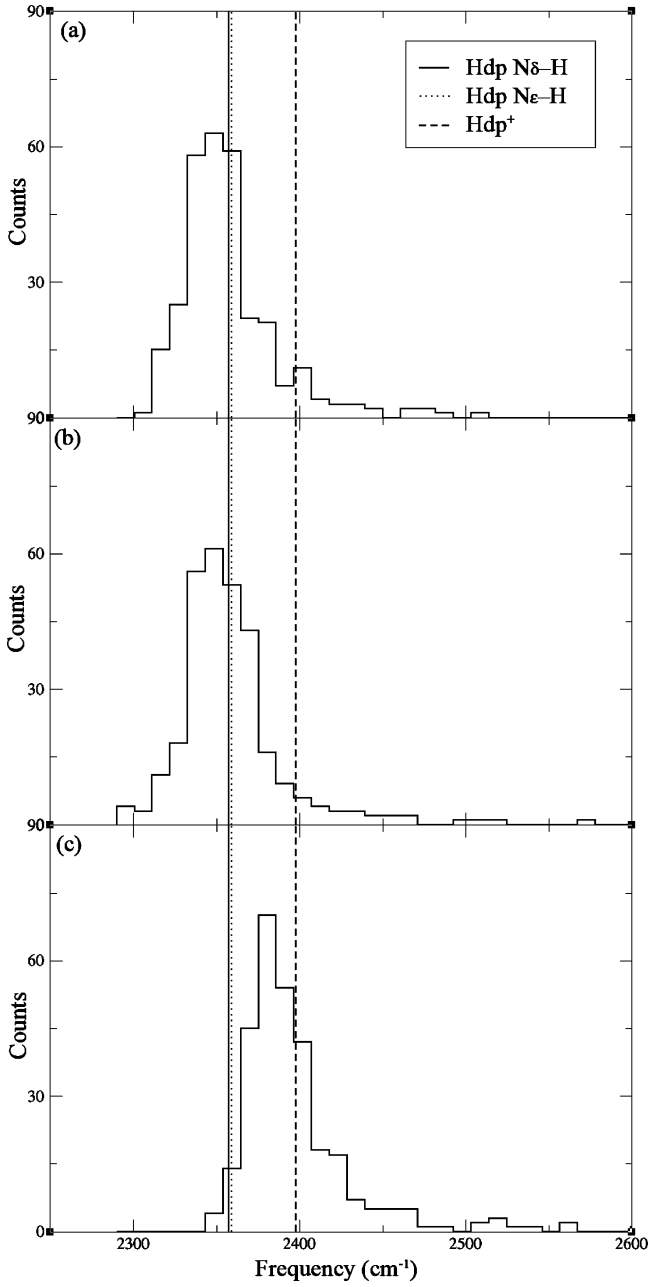

Figure 2. Frequency distributions of the $C_\varepsilon-D$ stretch mode of Hdp in aqueous solution: (a) Hdp N_δ-H, (b) Hdp N_ε-H, and (c) Hdp^+. The means of all three distributions are shown as vertical lines.

the ability of the $C_\delta-D$ and $C_\varepsilon-D$ to distinguish the protonated state from the deprotonated states is maintained. However, the ability of the probes to distinguish between the two neutral states is lost in aqueous solution.

Like in the gas-phase, the $C_\beta-D_2$ stretch frequencies are the least sensitive to changes in Hdp protonation state, with average shifts of $\sim$14 cm^{-1}. Nevertheless, such shifts would still likely be above the experimental detection limit, so $C_\beta-D_2$ is still a viable probe of histidine protonation state. Figure 3 shows frequency histograms for $C_\beta-D_2$ for the three Hdp protonation states, where the lowest energy eigenvalue for each snapshot was used to calculate ω_{sym}. Unlike in the gas-phase, in solution the $C_\beta-D_2$ probe frequencies red shift upon deprotonation to form Hdp N_ε-H,. Additionally, the average splitting between the asymmetric and symmetric stretches of the $C_\beta-D_2$ probe is increased in solution ($\sim$100 cm^{-1}) for all three Hdp protonation states. The response to deprotonation to form both Hdp N_ε-H and Hdp N_δ-H is now approximately the same (within $\sim$7 cm^{-1}) for $C_\beta-D_2$, so this probe is unlikely to be useful in distinguishing between the neutral states in solution.

One effect of solvating the Hdp molecule is a shift in the mean $C_\delta-D$, $C_\varepsilon-D$, and $C_\beta-D_2$ vibrational frequencies from their gas-phase values. To allow for a direct comparison, the gas-phase optimization and frequency calculations discussed here were performed using the 6-311++G(d, p) basis set (identical to the condensed-phase ONIOM calculations). For the carbon−deuterium vibrational probes on the ring, aqueous solvation results in a blue shift of the mean frequency for all three Hdp protonation states. The $C_\varepsilon-D$ and $C_\delta-D$ probes on Hdp^+ exhibit the largest shifts ($\sim$20 cm^{-1}), thus showing the most sensitivity to solvent stabilization of the charge on the ring. The $C_\delta-D$ and $C_\varepsilon-D$ probes in the neutral species show a smaller solvent-induced blue shift of $\sim$15 cm^{-1}, with one exception: the average $C_\delta-D$ frequency in Hdp N_ε-H showed a 2.5 cm^{-1} red shift upon solvation.

Solvation also affects the $C_\beta-D_2$ symmetric and asymmetric stretch vibrational frequencies. The asymmetric stretch frequency blue shifts significantly in all three molecules. Because the $C_\beta-D_2$ probe is not on the ring, it is not affected as much by the charge stabilization by the solvent in Hdp^+ as the $C_\varepsilon-D$ and $C_\delta-D$ probes. Instead, the largest solvent-induced asymmetric stretch frequency shift is in the Hdp N_δ-H molecule, which is protonated at the site closest to the probe. The $C_\beta-D_2$ symmetric stretch frequencies behave quite differently: the frequency in Hdp^+ blue shifts by a small amount, while the frequencies of the probe in the neutral Hdp molecules red shift slightly upon solvation. The average shift in the symmetric stretch due to solvation is only 3 cm^{-1}, while the average shift

TABLE 3: Mean Frequencies of the $C_\delta-D$, $C_\varepsilon-D$, and $C_\beta-D_2$, Vibrational Probes for the Three Protonation States of Hdp in Aqueous Solution[a]

Probe	Molecule	$\langle\omega\rangle$ (cm^{-1})		fwhm (cm^{-1})		$\Delta\omega_{deprotonation}$ (cm^{-1})		$\Delta\omega_{solvation}$ (cm^{-1})	
$C_\delta-D$	Hdp^+	2396.3		82				−18.4	
$C_\delta-D$	Hdp N_δ-H	2357.8		71		−38.5		−16.3	
$C_\delta-D$	Hdp N_ε-H	2357.2		74		−39.1		2.5	
$C_\varepsilon-D$	Hdp^+	2389.5		93				−20.9	
$C_\varepsilon-D$	Hdp N_δ-H	2357.2		70		−32.3		−14.7	
$C_\varepsilon-D$	Hdp N_ε-H	2358.8		98		−30.7		−15.0	
$C_\beta-D_2$	Hdp^+	2191.1	2288.4	68	91			−1.2	−31.6
$C_\beta-D_2$	Hdp N_δ-H	2173.7	2274.1	55	87	−17.4	−14.3	1.0	−43.2
$C_\beta-D_2$	Hdp N_ε-H	2180.2	2274.4	59	88	−10.8	−13.9	9.7	−17.6

[a] For the $C_\beta-D_2$ results, the symmetric stretch frequency is on the left and the asymmetric stretch frequency is on the right. The full-width at half-maximum (FWHM) is reported for each frequency distribution as FWHM = $2\sigma\sqrt{2\ln 2}$, where σ is the standard deviation of the calculated frequencies. The shift in the average frequency upon deprotonation is given as $\Delta\omega_{deprotonation} = \omega_{deprotonated} - \omega_{protonated}$, while the difference between the gas-phase calculated frequency and the mean solution-phase frequency is given as $\Delta\omega_{solvation} = \omega_{gas} - \omega_{condensed}$.

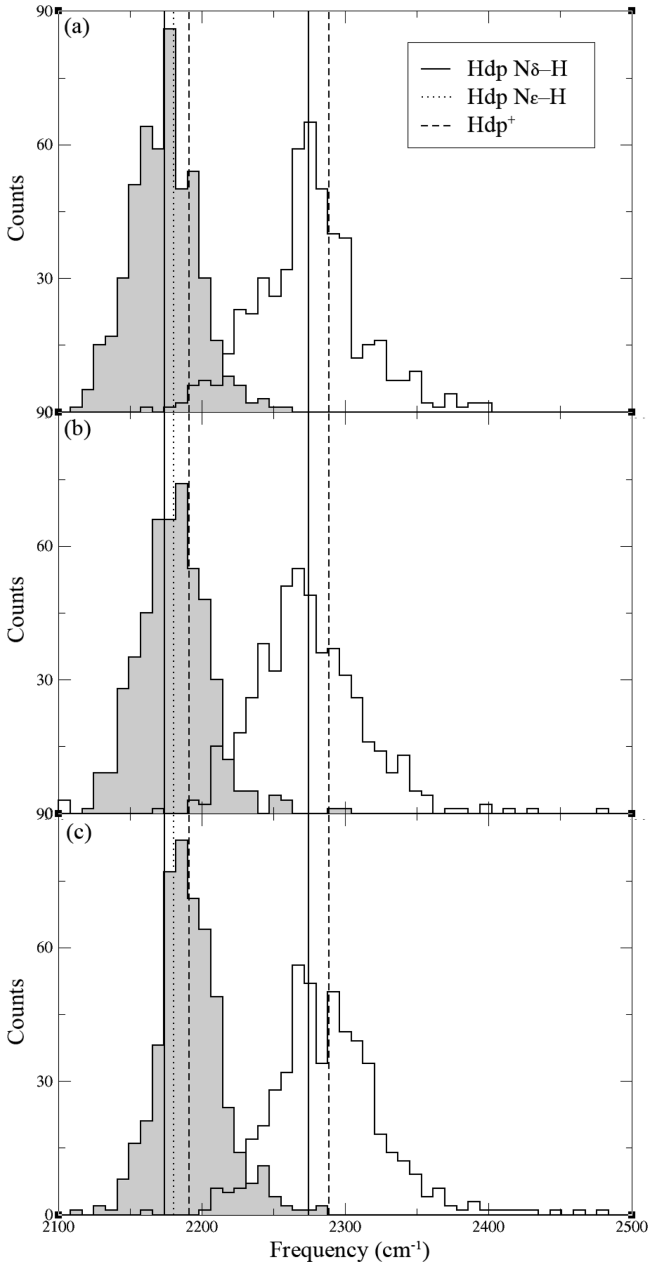

Figure 3. Frequency distributions of the symmetric (shaded) and asymmetric (white) $C_\beta-D_2$ modes of Hdp in aqueous solution: (a) Hdp N_δ-H, (b) Hdp N_ε-H, and (c) Hdp^+. The means of all six distributions are shown as vertical lines.

in the asymmetric stretch is considerably larger (33 cm^{-1}). The blue shifting of the asymmetric stretch frequency and red shifting of the symmetric stretch frequency create the large ($\sim$100 cm^{-1}) splitting between the modes in the condensed phase.

The widths of our calculated frequency distributions are considerably larger (50−100 cm^{-1}) than typical carbon−deuterium infrared absorption line shapes. The width of experimental infrared absorption line shapes is determined by several competing factors: inhomogeneous broadening, motional narrowing due to the dynamics of the fluctuating environment, and lifetime broadening. Our calculations produce only the inhomogeneous spectrum. However, a recent three-pulse photon echo investigation by Zimmerman et al. on carbon−deuterium-labeled leucines found frequency fluctuation dynamics that are consistent with substantial motional narrowing.[24] It is unlikely that the effects of motional narrowing would alter any of the conclusions for the sensitivity of carbon−deuterium probes of Hdp protonation state in aqueous solution.

IV. Concluding Remarks

We have comprehensively characterized the efficacy of carbon−deuterium vibrational probes as reporters of the protonation state of histidine. There are three viable locations for these vibrational probes: $C_\delta-D$, $C_\varepsilon-D$, and $C_\beta-D_2$. In the gas-phase, all three probes respond to deprotonation of Hdp^+. Moreover, $C_\delta-D$ and $C_\beta-D_2$ also exhibit an ability to distinguish between the two neutral Hdp molecules (Hdp N_ε-H and Hdp $N_\delta-H$). The calculated intensities of the $C_\delta-D$, $C_\varepsilon-D$, and $C_\beta-D_2$ stretches differ drastically between the charged and neutral Hdp molecules, which must be accounted for in determining relative populations of these species from experimental spectroscopic data. Hdp-d_4, which simultaneously contains all three carbon−deuterium probes, retains sensitivity to the changes in the Hdp protonation state. The C−D modes on the ring couple, forming symmetric and asymmetric stretches that have dramatic changes in frequency and intensity upon deprotonation of Hdp. While solvating the Hdp molecule in water does reduce the ability of the $C_\delta-D$ and $C_\beta-D_2$ vibrational probes to distinguish between the two neutral Hdp states, all three probes are still sensitive to the difference between the charged and neutral Hdp molecules. All of the frequencies are blue-shifted upon solvation, with the exception of the symmetric stretch of the $C_\beta-D_2$ probe which shows a small red shift. Future studies will investigate the sensitivity of carbon−deuterium vibrational probes to protonation states of titratable residues in protein environments. It will also be important to develop a quantitatively reliable model for the solvatochromic shift in frequency of C−D probes of protonation state. Such a model would allow the calculation of infrared absorption line shapes that contain the effects of motional narrowing, and to connect with nonlinear spectroscopic measurements.

Acknowledgment. We gratefully acknowledge the support of the National Science Foundation (CHE-0845736) and the American Chemical Society Petroleum Research Fund (PRF# 48432-G6).

References and Notes

(1) Anderson, D. E.; Becktel, W. J.; Dahlquist, F. W. *Biochemistry* **1990**, *29*, 2403.
(2) Forsyth, W. R.; Antosiewiez, J. M.; Robertson, A. D. *Proteins* **2002**, *48*, 388.
(3) Hu, C. Q.; Sturtevant, J. M.; Thomson, J. A.; Erickson, R. E.; Pace, C. N. *Biochemistry* **1992**, *31*, 4876.
(4) Meeker, A. K.; GarciaMoreno, B.; Shortle, D. *Biochemistry* **1996**, *35*, 6443.
(5) Pace, C. N.; Laurents, D. V.; Thomson, J. A. *Biochemistry* **1990**, *29*, 2564.
(6) Schwehm, J. M.; Fitch, C. A.; Dang, B. N.; Garcia-Moreno, B.; Stites, W. E. *Biochemistry* **2003**, *42*, 1118.
(7) Whitten, S. T.; Garcia-Moreno, B. *Biochemistry* **2000**, *39*, 14292.
(8) Yang, A. S.; Honig, B. *J. Mol. Biol.* **1993**, *231*, 459.
(9) Khurana, R.; Hate, A. T.; Nath, U.; Udgaonkar, J. B. *Protein Sci.* **1995**, *4*, 1133.
(10) Chen, H. M.; Chan, S. C.; Leung, K. W.; Wu, J. M.; Fang, H. J.; Tsong, T. Y. *FEBS J.* **2005**, *272*, 3967.
(11) Schenk, G.; Leeper, F. J.; England, R.; Nixon, P. F.; Duggleby, R. G. *Eur. J. Biochem.* **1997**, *248*, 63.
(12) Chan, P.; Warwicker, J. *BMC Biol.* **2009**, *7*, 10.
(13) Edgcomb, S. P.; Murphy, K. P. *Proteins* **2002**, *49*, 1.
(14) Plesniak, L. A.; Connelly, G. P.; Wakarchuk, W. W.; McIntosh, L. P. *Protein Sci.* **1996**, *5*, 2319.
(15) Wolff, N.; Deniau, C.; Letoffe, S.; Simenel, C.; Kumar, V.; Stojiljkovic, I.; Wandersman, C.; Delepierre, M.; Lecroisey, A. *Protein Sci.* **2002**, *11*, 757.

(16) Fitch, C. A.; Karp, D. A.; Lee, K. K.; Stites, W. E.; Lattman, E. E.; Garcia-Moreno, B. *Biophys. J.* **2002**, *82*, 3289.
(17) Takayama, Y.; Castaneda, C. A.; Chimenti, M.; Garcia-Moreno, B.; Iwahara, J. *J. Am. Chem. Soc.* **2008**, *130*, 6714.
(18) Kahyaoglu, A.; Jordan, F. *Protein Sci.* **2002**, *11*, 965.
(19) Pujato, M.; Navarro, A.; Versace, R.; Mancusso, R.; Ghose, R.; Tasayco, M. L. *Biochim. Biophys. Acta: Proteins Proteomics* **2006**, *1764*, 1227.
(20) Quijada, J.; Lopez, G.; Versace, R.; Ramirez, L.; Tasayco, M. L. *Biophys. Chem.* **2007**, *129*, 242.
(21) Griswold, I. J.; Dahlquist, F. W. *Nat. Struct. Biol.* **2002**, *9*, 567.
(22) Weinkam, P.; Zimmermann, J.; Sagle, L. B.; Matsuda, S.; Dawson, P. E.; Wolynes, P. G.; Romesberg, F. E. *Biochemistry* **2008**, *47*, 13470.
(23) Miller, C. S.; Corcelli, S. A. *J. Phys. Chem. B* **2009**, *113*, 8218.
(24) Zimmermann, J.; Gundogdu, K.; Cremeens, M. E.; Bandaria, J. N.; Hwang, G. T.; Thielges, M. C.; Cheatum, C. M.; Romesberg, F. E. *J. Phys. Chem. B* **2009**, *113*, 7991.
(25) Cremeens, M. E.; Zimmermann, J.; Yu, W.; Dawson, P. E.; Romesberg, F. E. *J. Am. Chem. Soc.* **2009**, *131*, 5726.
(26) Miller, C. S.; Ploetz, E. A.; Cremeens, M. E.; Corcelli, S. A. *J. Chem. Phys.* **2009**, 130.
(27) Mirkin, N. G.; Krimm, S. *J. Phys. Chem. A* **2004**, *108*, 10923.
(28) Mirkin, N. G.; Krimm, S. *J. Phys. Chem. A* **2007**, *111*, 5300.
(29) Mirkin, N. G.; Krimm, S. *J. Phys. Chem. B* **2008**, *112*, 15267.
(30) Arbely, E.; Arkin, I. T. *J. Am. Chem. Soc.* **2004**, *126*, 5362.
(31) Chin, J. K.; Jimenez, R.; Romesberg, F. E. *J. Am. Chem. Soc.* **2001**, *123*, 2426.
(32) Chin, J. K.; Jimenez, R.; Romesberg, F. E. *J. Am. Chem. Soc.* **2002**, *124*, 1846.
(33) Cremeens, M. E.; Fujisaki, H.; Zhang, Y.; Zimmermann, J.; Sagle, L. B.; Matsuda, S.; Dawson, P. E.; Straub, J. E.; Romesberg, F. E. *J. Am. Chem. Soc.* **2006**, *128*, 6028.
(34) Kinnaman, C. S.; Cremeens, M. E.; Romesberg, F. E.; Corcelli, S. A. *J. Am. Chem. Soc.* **2006**, *128*, 13334.
(35) Kumar, K.; Sinks, L. E.; Wang, J. P.; Kim, Y. S.; Hochstrasser, R. M. *Chem. Phys. Lett.* **2006**, *432*, 122.
(36) Naraharisetty, S. R. G.; Kasyanenko, V. M.; Zimmermann, J.; Thielges, M. C.; Romesberg, F. E.; Rubtsov, I. V. *J. Phys. Chem. B* **2009**, *113*, 4940.
(37) Naraharisetty, S. R. G.; Kurochkin, D. V.; Rubtsov, I. V. *Chem. Phys. Lett.* **2007**, *437*, 262.
(38) Sagle, L. B.; Zimmermann, J.; Dawson, P. E.; Romesberg, F. E. *J. Am. Chem. Soc.* **2004**, *126*, 3384.
(39) Sagle, L. B.; Zimmermann, J.; Dawson, P. E.; Romesberg, F. E. *J. Am. Chem. Soc.* **2006**, *128*, 14232.
(40) Sagle, L. B.; Zimmermann, J.; Matsuda, S.; Dawson, P. E.; Romesberg, F. E. *J. Am. Chem. Soc.* **2006**, *128*, 7909.
(41) Thielges, M. C.; Case, D. A.; Ronnesberg, F. E. *J. Am. Chem. Soc.* **2008**, *130*, 6597.
(42) Torres, J.; Arkin, I. T. *Biophys. J.* **2002**, *82*, 1068.
(43) Torres, J.; Kukol, A.; Arkin, I. T. *Biophys. J.* **2000**, *79*, 3139.
(44) Arkin, I. T. *Curr. Opin. Chem. Biol.* **2006**, *10*, 394.
(45) Bagchi, S.; Kim, Y. S.; Charnley, A. K.; Smith, A. B.; Hochstrasser, R. M. *J. Phys. Chem. B* **2007**, *111*, 3010.
(46) Barber-Armstrong, W.; Donaldson, T.; Wijesooriya, H.; Silva, R.; Decatur, S. M. *J. Am. Chem. Soc.* **2004**, *126*, 2339.
(47) Brauner, J. W.; Dugan, C.; Mendelsohn, R. *J. Am. Chem. Soc.* **2000**, *122*, 677.
(48) Bredenbeck, J.; Hamm, P. *J. Chem. Phys.* **2003**, *119*, 1569.
(49) Decatur, S. M. *Biopolymers* **2000**, *54*, 180.
(50) Decatur, S. M. *Acc. Chem. Res.* **2006**, *39*, 169.
(51) Fang, C.; Hochstrasser, R. M. *J. Phys. Chem. B* **2005**, *109*, 18652.
(52) Fang, C.; Wang, J.; Charnley, A. K.; Barber-Armstrong, W.; Smith, A. B.; Decatur, S. M.; Hochstrasser, R. M. *Chem. Phys. Lett.* **2003**, *382*, 586.
(53) Fang, C.; Wang, J.; Kim, Y. S.; Charnley, A. K.; Barber-Armstrong, W.; Smith, A. B.; Decatur, S. M.; Hochstrasser, R. M. *J. Phys. Chem. B* **2004**, *108*, 10415.
(54) Flach, C. R.; Cai, P.; Dieudonne, D.; Brauner, J. W.; Keough, K. M. W.; Stewart, J.; Mendelsohn, R. *Biophys. J.* **2003**, *85*, 340.
(55) Gordon, L. M.; Mobley, P. W.; Lee, W.; Eskandari, S.; Kaznessis, Y. N.; Sherman, M. A.; Waring, A. J. *Protein Sci.* **2004**, *13*, 1012.
(56) Hiramatsu, H.; Kitagawa, T. *Biochim. Biophys. Acta: Proteins Proteomics* **2005**, *1753*, 100.
(57) Huang, C. Y.; Getahun, Z.; Wang, T.; DeGrado, W. F.; Gai, F. *J. Am. Chem. Soc.* **2001**, *123*, 12111.
(58) Huang, R.; Kubelka, J.; Barber-Armstrong, W.; Silva, R.; Decatur, S. M.; Keiderling, T. A. *J. Am. Chem. Soc.* **2004**, *126*, 2346.
(59) Kim, Y. S.; Hochstrasser, R. M. *J. Phys. Chem. B* **2005**, *109*, 6884.
(60) Kim, Y. S.; Liu, L.; Axelsen, P. H.; Hochstrasser, R. M. *Proc. Natl. Acad. Sci. U.S.A.* **2008**, *105*, 7720.
(61) Kim, Y. S.; Wang, J. P.; Hochstrasser, R. M. *J. Phys. Chem. B* **2005**, *109*, 7511.
(62) Lin, Y. S.; Shorb, J. M.; Mukherjee, P.; Zanni, M. T.; Skinner, J. L. *J. Phys. Chem. B* **2009**, *113*, 592.
(63) Manor, J.; Mukherjee, P.; Lin, Y. S.; Leonov, H.; Skinner, J. L.; Zanni, M. T.; Arkin, I. T. *Structure* **2009**, *17*, 247.
(64) Moritz, R.; Fabian, H.; Hahn, U.; Diem, M.; Naumann, D. *J. Am. Chem. Soc.* **2002**, *124*, 6259.
(65) Mukherjee, P.; Kass, I.; Arkin, I.; Zanni, M. T. *Proc. Natl. Acad. Sci. U.S.A.* **2006**, *103*, 3528.
(66) Mukherjee, P.; Krummel, A. T.; Fulmer, E. C.; Kass, I.; Arkin, I. T.; Zanni, M. T. *J. Chem. Phys.* **2004**, *120*, 10215.
(67) Paul, C.; Axelsen, P. H. *J. Am. Chem. Soc.* **2005**, *127*, 5754.
(68) Paul, C.; Wang, J. P.; Wimley, W. C.; Hochstrasser, R. M.; Axelsen, P. H. *J. Am. Chem. Soc.* **2004**, *126*, 5843.
(69) Petty, S. A.; Adalsteinsson, T.; Decatur, S. M. *Biochemistry* **2005**, *44*, 4720.
(70) Petty, S. A.; Decatur, S. M. *J. Am. Chem. Soc.* **2005**, *127*, 13488.
(71) Petty, S. A.; Decatur, S. M. *Proc. Natl. Acad. Sci. U.S.A.* **2005**, *102*, 14272.
(72) Setnicka, V.; Huang, R.; Thomas, C. L.; Etienne, M. A.; Kubelka, J.; Hammer, R. P.; Keiderling, T. A. *J. Am. Chem. Soc.* **2005**, *127*, 4992.
(73) Silva, R.; Barber-Armstrong, W.; Decatur, S. M. *J. Am. Chem. Soc.* **2003**, *125*, 13674.
(74) Silva, R.; Kubelka, J.; Bour, P.; Decatur, S. M.; Keiderling, T. A. *Proc. Natl. Acad. Sci. U.S.A.* **2000**, *97*, 8318.
(75) Silva, R.; Nguyen, J. Y.; Decatur, S. M. *Biochemistry* **2002**, *41*, 15296.
(76) Smith, A. W.; Tokmakoff, A. *J. Chem. Phys.* **2007**, *126*, 045109.
(77) Starzyk, A.; Barber-Armstrong, W.; Sridharan, M.; Decatur, S. M. *Biochemistry* **2005**, *44*, 369.
(78) Torres, J.; Kukol, A.; Goodman, J. M.; Arkin, I. T. *Biopolymers* **2001**, *59*, 396.
(79) Venyaminov, S. Y.; Hedstrom, J. F.; Prendergast, F. G. *Proteins* **2001**, *45*, 81.
(80) Wang, J. P.; Chen, J. X.; Hochstrasser, R. M. *J. Phys. Chem. B* **2006**, *110*, 7545.
(81) Bandaria, J. N.; Dutta, S.; Hill, S. E.; Kohen, A.; Cheatum, C. M. *J. Am. Chem. Soc.* **2008**, *130*, 22.
(82) Cooper, I. B.; Barry, B. A. *Biophys. J.* **2008**, *95*, 5843.
(83) Lim, M. H.; Hamm, P.; Hochstrasser, R. M. *Proc. Natl. Acad. Sci. U.S.A.* **1998**, *95*, 15315.
(84) Oh, K. I.; Lee, J. H.; Joo, C.; Han, H.; Cho, M. *J. Phys. Chem. B* **2008**, *112*, 10352.
(85) Hill, S. E.; Bandaria, J. N.; Fox, M.; Vanderah, E.; Kohen, A.; Cheatum, C. M. *J. Phys. Chem. B* **2009**, *113*, 11505.
(86) Waegele, M. M.; Gai, F. *J. Phys. Chem. Lett.* **2010**, *1*, 781.
(87) Lindquist, B. A.; Furse, K. E.; Corcelli, S. A. *Phys. Chem. Chem. Phys.* **2009**, *11*, 8119.
(88) Boxer, S. G. *J. Phys. Chem. B* **2009**, *113*, 2972.
(89) Fang, C.; Bauman, J. D.; Das, K.; Remorino, A.; Arnold, E.; Hochstrasser, R. M. *Proc. Natl. Acad. Sci. U.S.A.* **2008**, *105*, 1472.
(90) Getahun, Z.; Huang, C. Y.; Wang, T.; De Leon, B.; DeGrado, W. F.; Gai, F. *J. Am. Chem. Soc.* **2003**, *125*, 405.
(91) Huang, C. Y.; Wang, T.; Gai, F. *Chem. Phys. Lett.* **2003**, *371*, 731.
(92) Krummel, A. T.; Zanni, M. T. *J. Phys. Chem. B* **2008**, *112*, 1336.
(93) Kurochkin, D. V.; Naraharisetty, S. R. G.; Rubtsov, I. V. *Proc. Natl. Acad. Sci. U.S.A.* **2007**, *104*, 14209.
(94) Mukherjee, S.; Chowdhury, P.; DeGrado, W. F.; Gai, F. *Langmuir* **2007**, *23*, 11174.
(95) Naraharisetty, S. R. G.; Kasyanenko, V. M.; Rubtsov, I. V. *J. Chem. Phys.* **2008**, *128*, 104502.
(96) Reddy, K. S.; Yonetani, T.; Tsuneshige, A.; Chance, B.; Kushkuley, B.; Stavrov, S. S.; Vanderkooi, J. M. *Biochemistry* **1996**, *35*, 5562.
(97) Schultz, K. C.; Supekova, L.; Ryu, Y. H.; Xie, J. M.; Perera, R.; Schultz, P. G. *J. Am. Chem. Soc.* **2006**, *128*, 13984.
(98) Silverman, L. N.; Pitzer, M. E.; Ankomah, P. O.; Boxer, S. G.; Fenlon, E. E. *J. Phys. Chem. B* **2007**, *111*, 11611.
(99) Suydam, I. T.; Boxer, S. G. *Biochemistry* **2003**, *42*, 12050.
(100) Suydam, I. T.; Snow, C. D.; Pande, V. S.; Boxer, S. G. *Science* **2006**, *313*, 200.
(101) Tucker, M. J.; Getahun, Z.; Nanda, V.; DeGrado, W. F.; Gai, F. *J. Am. Chem. Soc.* **2004**, *126*, 5078.
(102) Watson, M. D.; Gai, X. S.; Gillies, A. T.; Brewer, S. H.; Fenlon, E. E. *J. Phys. Chem. B* **2008**, *112*, 13188.
(103) Webb, L. J.; Boxer, S. G. *Biochemistry* **2008**, *47*, 1588.
(104) Yoshikawa, S.; Okeeffe, D. H.; Caughey, W. S. *J. Biol. Chem.* **1985**, *260*, 3518.
(105) Lindquist, B. A.; Corcelli, S. A. *J. Phys. Chem. B* **2008**, *112*, 6301.
(106) Lindquist, B. A.; Haws, R. T.; Corcelli, S. A. *J. Phys. Chem. B* **2008**, *112*, 13991.

(107) Choi, J.-H.; Oh, K.-I.; Lee, H.; Lee, C.; Cho, M. *J. Chem. Phys.* **2008**, *128*, 134506.
(108) Oh, K.-I.; Choi, J.-H.; Lee, J.-H.; Han, J.-B.; Lee, H.; Cho, M. *J. Chem. Phys.* **2008**, *128*, 154504.
(109) Maienschein-Cline, M. G.; Londergan, C. H. *J. Phys. Chem. A* **2007**, *111*, 10020.
(110) McMahon, H. A.; Alfieri, K. N.; Clark, K. A. A.; Londergan, C. H. *J. Phys. Chem. Lett.* **2010**, 850.
(111) Becke, A. D. *J. Chem. Phys.* **1993**, *98*, 5648.
(112) Miehlich, B.; Savin, A.; Stoll, H.; Preuss, H. *Chem. Phys. Lett.* **1989**, *157*, 200.
(113) Dunning, T. H. *J. Chem. Phys.* **1989**, *90*, 1007.
(114) Frisch, M. J.; Trucks, G. W.; Schlegel, H. B.; Scuseria, G. E.; Robb, M. A.; Cheeseman, J. R.; Montgomery Jr., J. A.; Vreven, T.; Kudin, K. N.; Burant, J. C.; Millam, J. M.; Iyengar, S. S.; Tomasi, J.; Barone, V.; Mennucci, B.; Cossi, M.; Scalmani, G.; Rega, N.; Petersson, G. A.; Nakatsuji, H.; Hada, M.; Ehara, M.; Toyota, K.; Fukuda, R.; Hasegawa, J.; Ishida, M.; Nakajima, T.; Honda, Y.; Kitao, O.; Nakai, H.; Klene, M.; Li, X.; Knox, J. E.; Hratchian, H. P.; Cross, J. B.; Bakken, V.; Adamo, C.; Jaramillo, J.; Gomperts, R.; Stratmann, R. E.; Yazyev, O.; Austin, A. J.; Cammi, R.; Pomelli, C.; Ochterski, J. W.; Ayala, P. Y.; Morokuma, K.; Voth, G. A.; Salvador, P.; Dannenberg, J. J.; Zakrzewski, V. G.; Dapprich, S.; Daniels, A. D.; Strain, M. C.; Farkas, O.; Malick, D. K.; Rabuck, A. D.; Raghavachari, K.; Foresman, J. B.; Ortiz, J. V.; Cui, Q.; Baboul, A. G.; Clifford, S.; Cioslowski, J.; Stefanov, B. B.; Liu, G.; Liashenko, A.; Piskorz, P.; Komaromi, I.; Martin, R. L.; Fox, D. J.; Keith, T.; Al-Laham, M. A.; Peng, C. Y.; Nanayakkara, A.; Challacombe, M.; Gill, P. M. W.; Johnson, B.; Chen, W.; Wong, M. W.; Gonzalez, C.; Pople, J. A. *Gaussian 03, Revision C.02*; Gaussian Inc.: Wallingford, CT, 2004.
(115) Case, D. A.; Darden, T. A.; Cheatham, T. E.; Simmerling, C. L.; Wang, J.; Duke, R. E.; Luo, R.; Merz, K. M.; Pearlman, D. A.; Crowley, M.; Walker, R. C.; Zhang, W.; Wang, B.; Hayik, S.; Roitberg, A.; Seabra, G.; Wong, K. F.; Paesani, F.; Wu, X.; Brozell, S.; Tsui, V.; Gohlke, H.; Yang, L.; Tan, C.; Mongan, J.; Hornak, V.; Cui, G.; Beroza, P.; Mathews, D. H.; Schafmeister, C.; Ross, W. S.; Kollman, P. A. *AMBER 9*; University of California, San Francisco: San Francisco, 2006.
(116) Hornak, V.; Abel, R.; Okur, A.; Strockbine, B.; Roitberg, A.; Simmerling, C. *Proteins* **2006**, *65*, 712.
(117) Svensson, M.; Humbel, S.; Froese, R. D. J.; Matsubara, T.; Sieber, S.; Morokuma, K. *J. Phys. Chem.* **1996**, *100*, 19357.
(118) Tomasi, J.; Mennucci, B.; Cammi, R. *Chem. Rev.* **2005**, *105*, 2999.
(119) Vreven, T.; Mennucci, B.; da Silva, C. O.; Morokuma, K.; Tomasi, J. *J. Chem. Phys.* **2001**, *115*, 62.
(120) Cappelli, C.; Mennucci, B. *J. Phys. Chem. B* **2008**, *112*, 3441.
(121) Mennucci, B.; Martinez, J. M. *J. Phys. Chem. B* **2005**, *109*, 9818.
(122) Mennucci, B.; Martinez, J. M. *J. Phys. Chem. B* **2005**, *109*, 9830.
(123) Cappelli, C.; Monti, S.; Scalmani, G.; Barone, V. *J. Chem. Theory Comput.* **2010**, *6*, 1660.

JP1028596